Determining the thermal diffusivity and the principal directions on anisotropic moving samples with laser-spot thermography

Agustín Salazar*, Mateu Colom and Arantza Mendioroz

Departamento de Física Aplicada I, Escuela de Ingeniería de Bilbao, Universidad del País Vasco UPV/EHU, Plaza Ingeniero Torres Quevedo 1, 48013 Bilbao, Spain

*Corresponding author, E-mail address: agustin.salazar@ehu.es

ABSTRACT

We propose a method to measure the thermal diffusivity of (an)isotropic samples moving at constant speed using laser-spot thermography with continuous illumination. The method does not require previous knowledge of the principal directions and can be applied whichever their orientation with respect to the direction of motion. We demonstrate analytically that any radial temperature profile crossing the center of the laser spot fulfills a linear relation with the distance to the laser spot, whose slope depends on the thermal diffusivity, on the sample speed and on the angle of the profile with respect the sample motion. A multi-linear fitting of the temperature profiles at several angles provides a reliable method to obtain the thermal diffusivity. Experiments performed on reference samples, both isotropic and anisotropic, confirm the validity of the method to provide accurate and precise thermal diffusivity values and to identify the thermal principal directions.

Keywords: thermal diffusivity, flying-spot thermography, laser-spot thermography, linear relations, moving samples.

1. INTRODUCTION

Thermal diffusivity is the physical quantity that governs the heat diffusion equation. Measuring it in a reliable way is of great interest in both science and engineering heat transfer problems. In the last decades several non-contact methods have been proposed to measure the thermal diffusivity of a wide variety of solids according to their geometry: bulk, thin films, wires, graded multilayers, etc. See Ref. [1] for a recent review.

Laser-spot thermography is a powerful tool to measure the in-plane thermal diffusivity of solids (for a recent tutorial see [2] and references therein). It consists in heating the sample with a tightly focused laser beam and recording the surface temperature with an infrared video camera. Two time regimes of the laser beam have been explored: an amplitude modulated laser [3,4] and a pulsed laser [5-7]. If the sample is opaque, a fraction of the laser energy is absorbed at the position of the laser spot at the sample surface, producing a temperature rise with respect to the room temperature. Then, heat diffuses in the material producing a radial temperature gradient. The further the heat diffuses, the greater its thermal diffusivity.

Recently, laser-spot thermography has been proposed to measure the in-plane thermal diffusivity of samples moving at constant speed [8-11], as it is the case of in-line inspection in factories, where local changes in the thermal properties must be detected in real time, without stopping the production chain. Alternatively, for the fast inspection of big samples that stay at rest, the laser spot scans the sample at constant speed. This so-called flying-spot thermography has been used to measure the in-plane thermal diffusivity of complex parts [12-15].

In laser-spot lock-in thermography, where the laser power is harmonically modulated at a given frequency, it is well-known that when both laser spot and sample are at rest, the natural logarithm of the temperature decreases linearly as the distance from the centre of the laser spot increases. The slope of this linear relation gives the in-plane thermal diffusivity of the sample, provided the modulation frequency is known [3,4]. Recently, in the case of continuous illumination of moving samples, we demonstrated that there are linear relations between two specific temperature profiles (in the longitudinal and transverse directions with respect to the direction of the sample motion), and the distance to the laser spot [8]. The slopes of these straight lines are related to the in-plane thermal diffusivity of the sample, provided the sample speed is known. In the case of anisotropic samples, this method requires not only knowledge of the principal directions but also necessitates that the sample moves parallel to one of the principal directions. The method was tested by measuring the thermal diffusivity of reference samples. For good thermal conductors this linear method gave very good results. However, for thermal insulators we were unable to find accurate diffusivity values due to the lack of linearity of the longitudinal and transverse profiles (see Table 1 in Ref. [8]).

In this work, we find an analytical expression for the surface temperature of a sample moving at constant speed when it is illuminated by a tightly focused laser beam. Both isotropic and anisotropic samples are considered. These analytical equations demonstrate that all radial temperature profiles behave linearly, not just the longitudinal and transverse ones. The slopes of these linear relations satisfy a simple equation that depends on the sample thermal diffusivity and speed, and on the angle of the profile with respect to the direction of the sample motion. Accordingly, we propose to obtain the in-plane thermal diffusivity of the sample from a multi-linear fitting of the slopes obtained at several angles, thus reducing systematic errors and achieving better accuracy and precision. This method is especially useful when the material is anisotropic and the directions of the principal axes are unknown. This can be the case in in-line monitoring of industrial anisotropic products in a production chain, for both thermal properties and anisotropy orientation control, when the direction of motion does not necessarily coincide with the direction of the principal axes. In that case, we obtain the in-plane principal diffusivities together with the orientation of the principal axes. This method has been tested on

three reference samples: a thermal insulator, a good thermal conductor and an anisotropic composite.

2. THEORY

2.1. Isotropic materials

We start considering an isotropic and opaque sample whose surface is illuminated by a CW laser spot moving along the x-axis at constant speed v. The laser spot, which is tightly focused so its size is negligible, was turned on at $t_o < 0$ and is crossing the origin of coordinates just at $t = 0$. The scheme of the problem is shown in Fig. 1a.

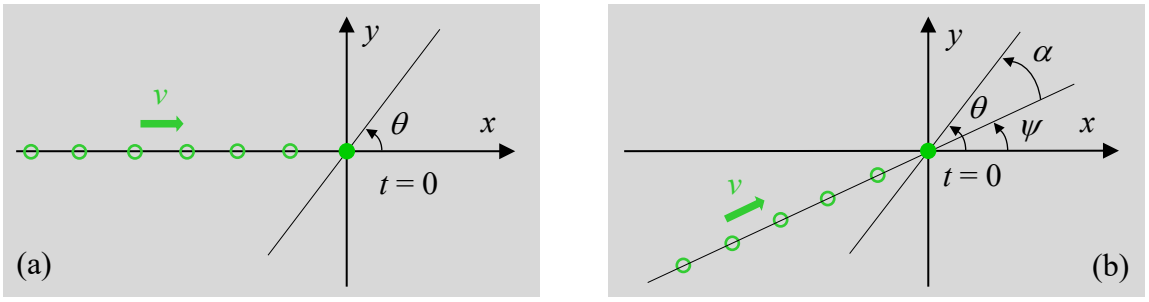

FIG. 1. Sample surface illuminated by a CW laser spot moving at constant speed v, (a) along the x-axis and (b) along a direction making an angle ψ with respect to the x-axis. The laser is at the origin of coordinates at $t = 0$.

If the laser spot was turned on at $t_o = -\infty$, the steady state is already reached when the laser spot is crossing the origin of coordinates ($t = 0$). Under these conditions, and neglecting heat losses by convection and radiation, the surface temperature has a time independent analytical expression (see Eq. (2) on page 267 in Ref. [16])

$$T(x,y) = \frac{\eta P_o}{2\pi K}\frac{1}{r}e^{-\frac{v(r+x)}{2D}}, \tag{1}$$

where $r = \sqrt{x^2 + y^2}$, P_o is the laser power, η is the power fraction absorbed by the sample, K is the thermal conductivity and D the thermal diffusivity.

In particular, the temperature profile along a straight line crossing the origin of coordinates and making an angle θ with respect to the x-axis (see Fig. 1a) is given by

$$T(r,\theta) = \frac{\eta P_o}{2\pi K}\frac{1}{r}e^{-\frac{vr(1+\cos\theta)}{2D}}. \tag{2}$$

According to Eq. (2), the natural logarithm of the product of the temperature and the distance to the laser spot, $\ln(Tr)$, has a linear relation as a function of r

$$\ln(Tr) = \ln\left(\frac{\eta P_o}{2\pi K}\right) - \frac{v}{2D}(1+\cos\theta)r, \tag{3}$$

whose slope verifies

$$m_\theta = -\frac{v}{2D}(1+\cos\theta), \tag{4}$$

indicating that it varies from $-v/D$ to 0 as the angle sweeps the 0º - 180º range. By measuring the slope at different angles θ with respect to the direction of the laser motion, the thermal diffusivity of the sample can be obtained accurately, as long as the laser speed is known.

2.2. Anisotropic materials

If the sample is anisotropic and its principal axes coincide with the coordinates axes, in the steady state the surface temperature has an analytical expression

$$T(x,y)=\frac{\eta P_o}{2\pi\varepsilon_z}\frac{1}{\sqrt{x^2D_y+y^2D_x}}e^{-\frac{v}{2}\left(\frac{x}{D_x}+\sqrt{\frac{x^2D_y+y^2D_x}{D_x^2D_y}}\right)}, \tag{5}$$

where ε_z is the thermal effusivity of the sample along the z-axis and D_x and D_y are the principal diffusivities along the x-axis and y-axis, respectively. The temperature profile along a straight line crossing the origin of coordinates and making an angle θ with respect to the x-axis is given by

$$T(r,\theta)=\frac{\eta P_o}{2\pi\varepsilon_z}\frac{1}{r}\frac{1}{\sqrt{D_x\sin^2\theta+D_y\cos^2\theta}}e^{m_\theta r}. \tag{6}$$

From Eq. (6) it can be seen that the natural logarithm of the product of the temperature and the distance to the laser spot, $\ln(Tr)$, has a linear relation as a function of r

$$\ln(Tr)=\ln\left(\frac{\eta P_o}{2\pi\varepsilon_z}\frac{1}{\sqrt{D_x\sin^2\theta+D_y\cos^2\theta}}\right)+m_\theta r, \tag{7}$$

where the slope verifies

$$m_\theta=-\frac{v}{2}\left[\frac{\cos\theta}{D_x}+\sqrt{\frac{1}{D_x}\left(\frac{\sin^2\theta}{D_y}+\frac{\cos^2\theta}{D_x}\right)}\right]. \tag{8}$$

This slope takes values of $-\frac{v}{D_x}$, $-\frac{v}{2\sqrt{D_xD_y}}$ and 0 for angles $\theta=0$º, 90º, and 180º, respectively. As in the case of isotropic samples, by measuring the slope at different angles θ with respect to the direction of the laser movement, the in-plane thermal diffusivities of the sample, D_x and D_y, can be obtained accurately.

Now, let us consider the most general case where the laser spot is moving along a direction making an angle ψ with respect to the principal axis x (see Fig. 1b). The temperature profile along an arbitrary line crossing the origin of coordinates and making an angle θ with respect to the x-axis can be obtained straightforwardly from Eq. (5) and is given by

$$T(r,\theta)=\frac{\eta P_o}{2\pi\varepsilon_z}\frac{1}{r}\frac{1}{\sqrt{D_x\sin^2\theta+D_y\cos^2\theta}}e^{m_{\theta,\psi}r}, \tag{9}$$

so $\ln(Tr)$ has a linear relation as a function of r

$$\ln(Tr)=\ln\left(\frac{\eta P_o}{2\pi\varepsilon_z}\frac{1}{\sqrt{D_x\sin^2\theta+D_y\cos^2\theta}}\right)+m_{\theta,\psi}r, \tag{10}$$

where the slope verifies

$$m_{\theta,\psi}=-\frac{v}{2}\left[\frac{\cos\theta\cos\psi}{D_x}+\frac{\sin\theta\sin\psi}{D_y}+\sqrt{\left(\frac{\sin^2\psi}{D_y}+\frac{\cos^2\psi}{D_x}\right)\left(\frac{\sin^2\theta}{D_y}+\frac{\cos^2\theta}{D_x}\right)}\right]. \tag{11}$$

If the orientation of the principal axes are known, ψ is a given parameter, so by measuring the slope of the temperature profiles at several angles θ, the in-plane principal thermal diffusivities can be obtained. Anyway, Eq. (11) is especially useful when the directions of the principal axes of the anisotropic material are unknown. In that case, we only control the angle that the selected profile makes with the direction of motion, $\alpha = \theta - \psi$, so in Eq. (11) we replace θ by $\psi + \alpha$. Accordingly, by measuring the slope of the temperature profiles at several angles α, we obtain D_x and D_y together with the orientation of the principal axes ψ.

2.3. Analysis and discussion

In Fig. 2 we show the calculations of the isotherms of the natural logarithm of the surface temperature for an anisotropic sample ($D_x = 4$ mm^2/s, $D_y = 1$ mm^2/s) when the laser spot is moving at $v = 10$ mm/s. In Fig. 2a the laser spot is moving along the x direction. As it is a principal axis, the contour plots are symmetric with respect to this axis. In Fig. 2b the motion of the laser spot is along a direction making an angle $\psi = 45^\circ$. As can be observed, the symmetry of the isotherms is broken.

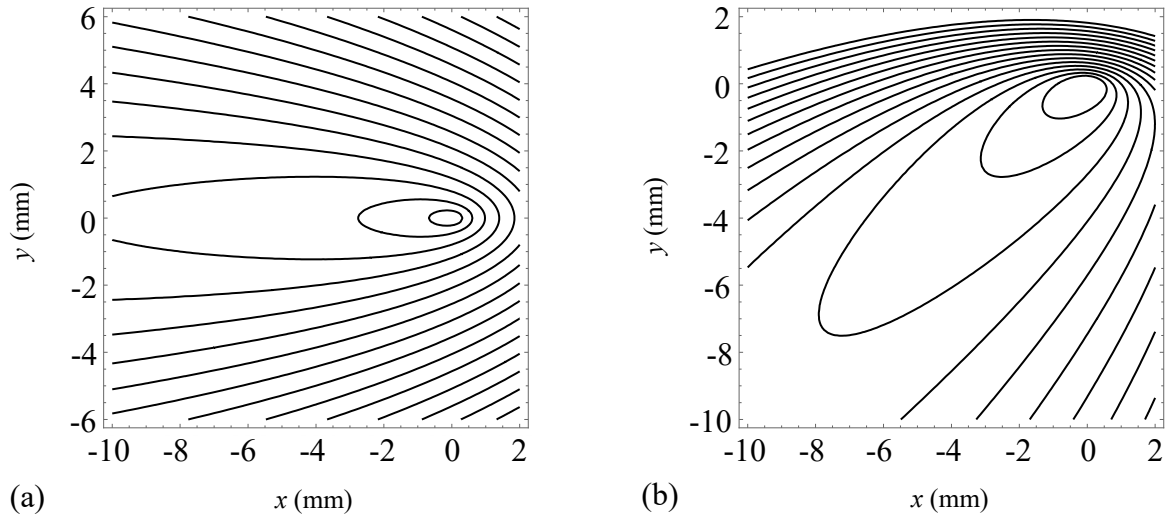

Fig. 2. Calculated contour plots of ln(T) for an anisotropic sample ($D_x = 4$ mm^2/s, $D_y = 1$ mm^2/s) when the laser spot is moving at $v = 10$ mm/s, (a) along the x-axis and (b) along a direction at $\psi = 45^\circ$.

Figure 3a shows the behavior of the slope of the temperature profiles for an anisotropic sample that is illuminated by a laser spot moving at 10 mm/s along the principal x-axis. This calculation has been performed using Eq. (8). Three materials have been considered according to their principal thermal diffusivities. The black line corresponds to an isotropic sample with $D_x = D_y = 4$ mm^2/s. As can be observed, the slope follows a sinusoidal curve. The red line stands for an anisotropic sample where the thermal diffusivity along the x-axis is four times larger than the thermal diffusivity along the y-axis: $D_x = 4$ mm^2/s, $D_y = 1$ mm^2/s. On the contrary, the blue line corresponds to an anisotropic sample where the thermal diffusivity along the x-axis is four times smaller than the thermal diffusivity along the y-axis: $D_x = 4$ mm^2/s, $D_y = 16$ mm^2/s. In all cases the slope is zero for $\theta = 180^\circ$. However, the minimum is reached at $\theta = 0^\circ$ when $D_x > D_y$, while for $D_x < D_y$ the minimum appears at an intermediate angle $0^\circ < \theta < 90^\circ$.

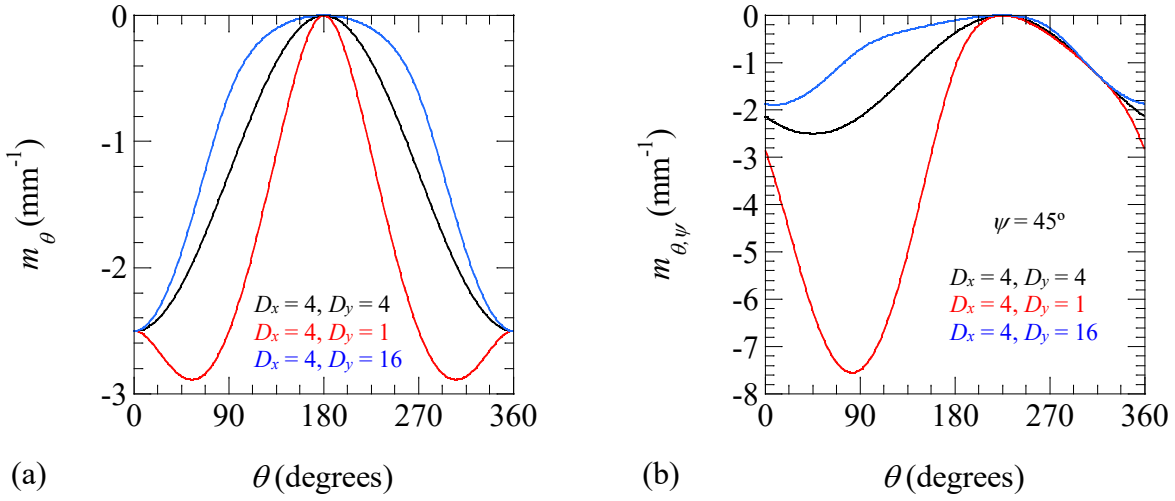

FIG. 3. Evolution of the slope of ln(*Tr*) for an anisotropic sample illuminated by a laser spot moving at $v = 10$ mm/s. (a) The laser spot is moving along the principal *x*-axis. (b) The laser is moving along a direction making an angle $\psi = 45^o$ with respect to the principal *x*-axis. Diffusivities are given in mm^2/s.

In Fig. 3b we show the behavior of the slope of the temperature profiles for the same conditions as in Fig. 3a, but in this case the laser spot is moving in a direction making an angle $\psi = 45^o$ with respect to the principal *x*-axis. This calculation has been performed using Eq. (11). The black line, which corresponds to an isotropic sample, describes the same sinusoidal shape as in Fig. 3a, but shifted by an angle of 45º. For anisotropic samples, the behavior is more complicated since, as shown in Fig. 2b, the symmetry is broken. Anyway, there is always a null slope at $\theta = 180^o + \psi$, in this example $\theta = 225^o$.

To conclude this section let us stress that the slopes of the surface temperature profiles given by Eqs. (4), (8) and (11) provide a simple method to measure the thermal diffusivity of solids illuminated by a laser spot moving at constant speed. Moreover, according to the relativity principle, these three equations are also valid in the complementary experimental configuration, where the laser is at rest while the sample is moving at constant speed. This is the case of in-line production in factories, where the thermal properties must be measured in real time, without stopping the production chain. Finally, let us remark that although these three equations have been obtained under ideal conditions (negligible spot size and absence of heat losses) the expressions of the slopes remain unchanged when the laser spot has a finite size and when realistic values of the heat loss coefficients by convection and radiation are taken into account [8].

3. EXPERIMENTAL RESULTS AND DISCUSSION

Figure 4 shows the scheme of the laser-spot thermography setup with the sample moving at constant speed. A CW laser (532 nm, up to 6 W) of Gaussian profile is focused on the sample surface by means of a 10 cm focal length lens to a radius of about 50 μm. A mirror-like polished Ge window, which is opaque to visible light, is used to direct the laser beam perpendicularly to the specimen. At the same time, this Ge window is transparent to the IR radiation allowing the thermal energy emitted by the sample to reach the IR video camera. Anyway, due to the high refractive index of Ge, the window is covered by an anti-reflection coating to enhance IR

transmission. To minimize the heating of the Ge window, which would contribute to the observed temperature increase (in addition to the one coming from the sample) the laser remains on for only the few seconds it takes for the sample to cross the field of view (FOV) of the camera. An IR video camera (3-5 μm, 320×256 px, 30 μm pitch, up to 380 images/s at full frame, NETD 20 mK) records the temperature field of the sample surface. A macro lens produces a magnification ratio 1:1, i.e. each pixel of the detector senses the average temperature over a 30 μm square of the sample, with a FOV of 9.60 mm x 7.68 mm. The sample is mounted on a dynamic system (cart + track) that is coupled to an electric engine to move the cart at constant speed in the range between 1 and 150 mm/s. The sample speed is obtained by dividing the length of the sample by the time lapse between the entrance and the exit of one end of the sample in the FOV of the camera (number of frames divided by the frame rate of the camera). Proceeding in this way, the sample speed is measured with an uncertainty of less than 0.2%.

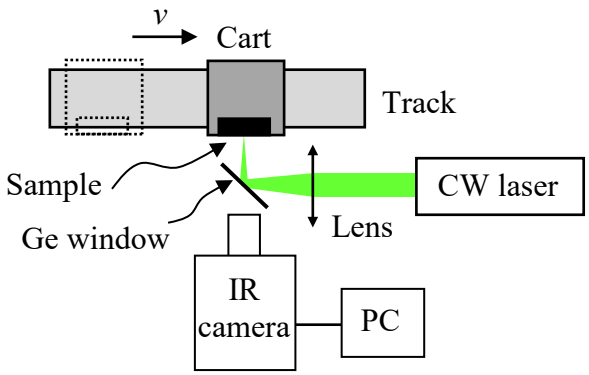

Fig. 4. Scheme of the laser-spot thermography setup on a moving sample.

To test the validity of the method proposed in this work, based on the linear behavior of the temperature profiles, we have performed laser-spot thermography measurements on three samples at several speeds. The first one is a poor thermal conductor, polyether-ether-ketone (PEEK). This is a high performance amorphous thermoplastic with high temperature resistance. Thin PEEK films are transparent, but specimens thicker than 0.5 mm are quasi-opaque and grey coloured. PEEK has been used for years in our laboratory as a reference material for thermal diffusivity measurements. Applying different photothermal techniques (flash method, photopyroelectric technique and lock-in thermography) we have obtained a thermal diffusivity value in the range 0.19 - 0.21 mm^2/s. The dimensions of the specimen used in this work are 100 mm × 40 mm × 4 mm. The sample was covered by a thin graphite layer to guarantee its complete opacity. The second material is an intermediate thermal conductor, stainless steel AISI-304. This is an iron based alloy which contains 18% de Cr and 8% Ni. The size of the specimen we have analyzed in this work is 200 mm × 50 mm × 40 mm. Due to the high reflectivity of the surface we deposited a thin graphite layer to enhance both the laser absorption and the emissivity at IR wavelengths. Using both lock-in thermography and the flash method we have obtained a thermal diffusivity value in the range 3.8 - 4.1 mm^2/s. The last specimen is an anisotropic sample, a carbon fiber reinforced polymer (CFRP), which is a composite made of unidirectional carbon fibers embedded in an epoxy matrix. In this sample heat conduction in the direction of the carbon fibers is greatly enhance with respect to the perpendicular directions. The sample we have dealt with is a parallelepiped with size 100 mm × 50 mm × 5 mm. As it is opaque and features a high IR emissivity we performed thermography measurements without covering it with graphite. Lock-in thermography measurements lead~~s to a~~ thermal diffusivity

values of 2.9 ± 0.1 mm^2/s and 0.40 ± 0.02 mm^2/s, in the directions parallel and perpendicular to the fibers, respectively.

The IR video camera records a film as the sample is moving in front of the camera along the horizontal axis. To enhance the signal to noise ratio, we work with a thermogram, which is the average of several hundreds of successive thermograms in the recorded film, after the steady state has been reached.

In the upper row of Fig. 5 we show the averaged thermograms of ln(T) for an AISI-304 specimen at three sample speeds v = 5.50, 21.4 and 81.6 mm/s. As can be observed, the higher the speed, the larger the elongation of the isotherms. In Fig. 5a we show the experimental profiles of ln(Tr) versus the distance to the center of the laser spot for an AISI-304 sample moving at v = 41.2 mm/s at several angles θ with respect to the direction of the sample motion. Dots are the experimental data whereas the continuous lines are the best linear fits from which the slopes are obtained. We took data every 10º, i.e. 36 profiles, but for the sake of clarity, only some of them are plotted. Figure 5b is the plot of the fitted slopes as a function of the angle θ together with the fitting to Eq. (4) using a Levenberg-Marquardt algorithm. From this fitting a thermal diffusivity value D = 3.8 ± 0.2 mm^2/s is obtained. The errors bars in Fig. 5b corresponds to the standard deviation of the linear fits. We have repeated the same procedure for six sample speeds: 5.50, 10.9, 21.4, 41.2, 60.4 and 81.6 mm/s. The retrieved thermal diffusivity values are summarized in Table 1. As can be observed, all of them are consistent and agree very well with our own values using other photothermal techniques on the sample at rest and with the value reported in the literature, within the statistical uncertainty [17]. Note that the uncertainty for the higher speeds is a bit larger due to the lack of spatial resolution of our IR camera. Actually, at high speeds the shape of the thermogram is very elongated and therefore the temperature profiles contain fewer points than at low speeds, which diminishes the reliability of the results.

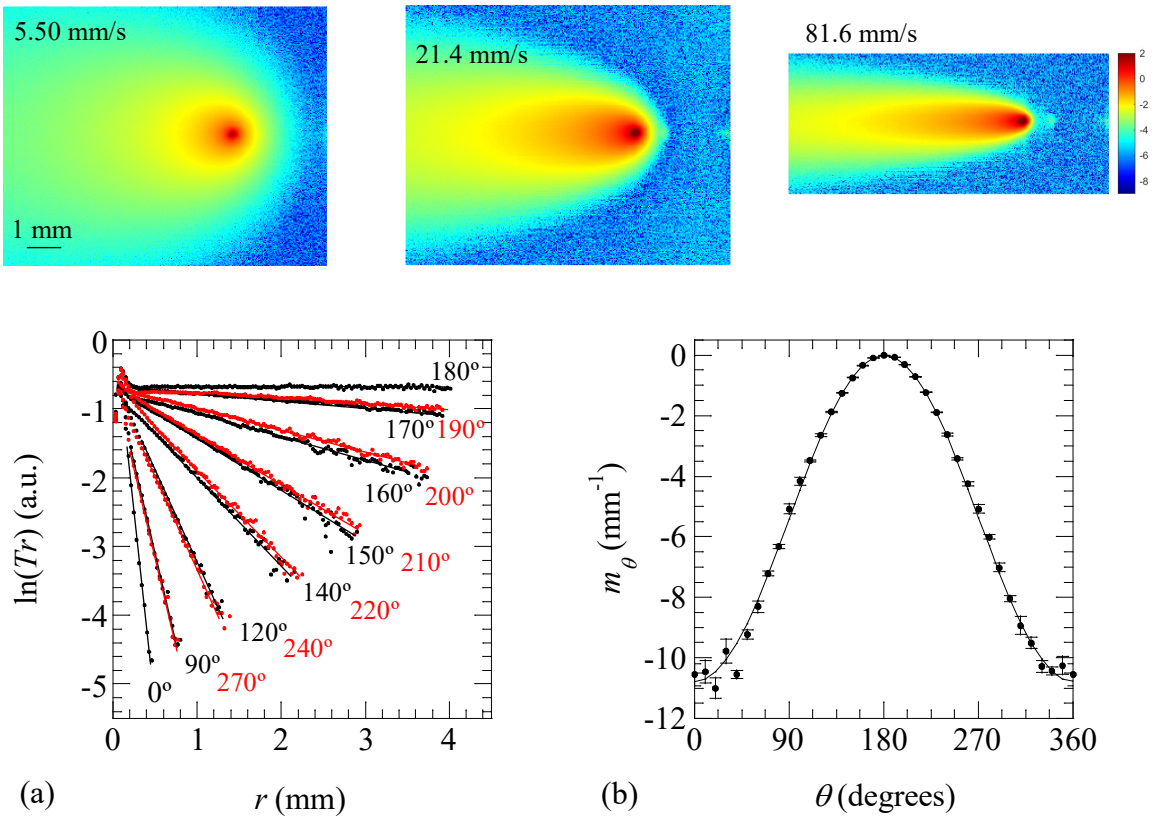

Fig. 5. Upper row: averaged thermograms of ln(T) for an AISI-304 specimen corresponding to three sample speeds. Lower row: (a) Experimental profiles of ln(Tr) as a function of the distance

to the laser spot for AISI-304 at several angles with respect to the direction of the sample motion, for v = 41.2 mm/s. Dots are the experimental data and the straight lines are the linear fits. (b) Experimental slopes versus angle θ corresponding to the linear fits of Fig. 5(a). The continuous line is the fit using Eq. (4).

The averaged thermograms of ln(T) for a PEEK plate at v = 0.49 and 4.30 mm/s are plotted in the upper row of Fig. 6. As the thermal diffusivity of PEEK is about 20 times smaller than that of AISI-304, the PEEK isotherms at 4.30 mm/s are as elongated as AISI-304 at v = 81.6 mm/s. In Fig. 6a we show the experimental profiles of ln(Tr) as a function of the distance to the laser spot for the PEEK sample moving at v = 1.00 mm/s at several angles θ. Dots are the experimental data and the continuous lines are the linear fits from which the slopes are obtained. Figure 6b represents the plot of the fitted slopes as a function of the angle θ together with the fitting to Eq. (4) using a Levenberg-Marquardt algorithm. From this fitting a thermal diffusivity value D = 0.21 ± 0.1 mm^2/s is obtained. The errors bars in Fig. 6b corresponds to the standard deviation of the linear fits. We have repeated the same procedure for three sample speeds: 0.49, 1.00 and 4.30 mm/s. These results are summarized in Table 1. As can be observed, all of them are consistent and agree with our own values using other photothermal techniques on the sample at rest and with the value reported in the literature within the statistical uncertainty [18]. For speeds higher than 5 mm/s the thermograms are so elongated that the temperature profiles contain just a few points, leading to unreliable thermal diffusivity values. Measuring thermal insulators at higher speeds would require a high resolution infrared camera.

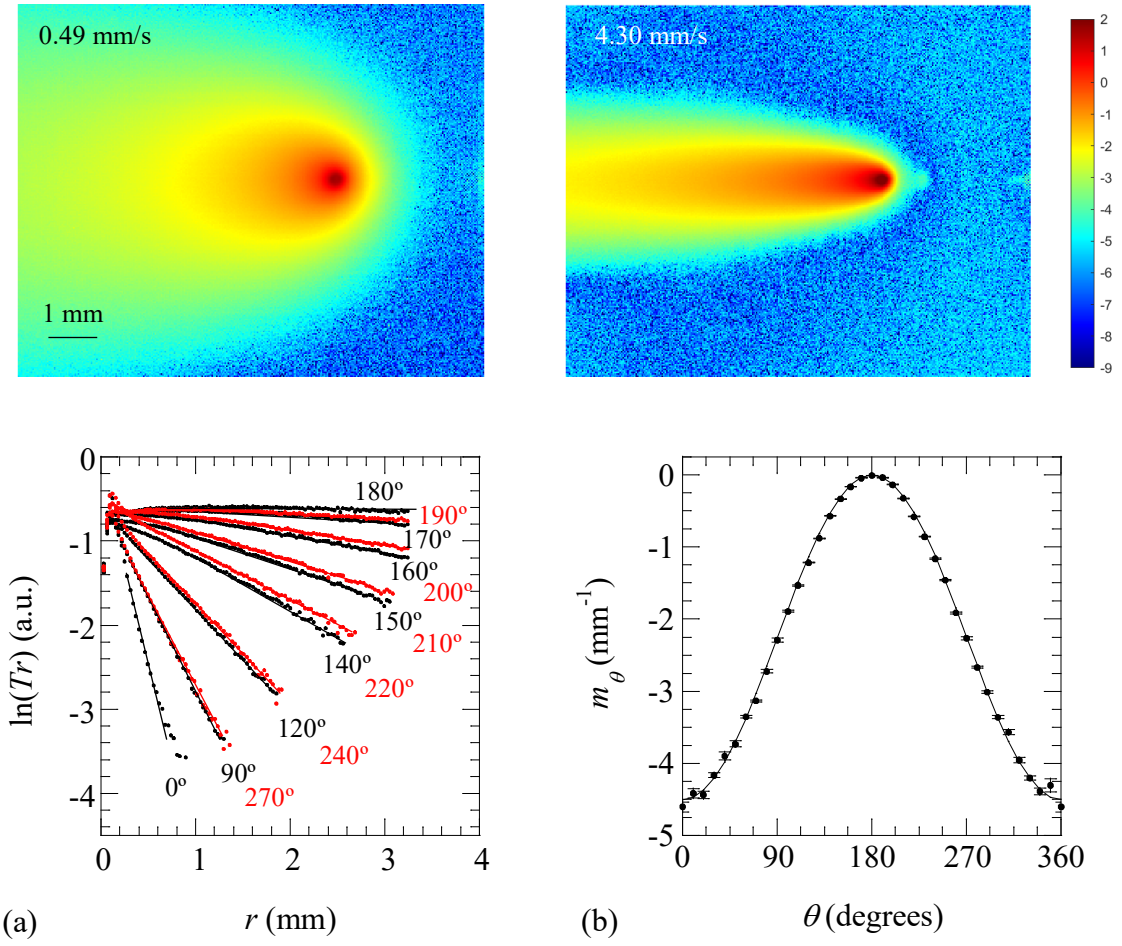

Fig. 6. Upper row: averaged thermograms of ln(T) for a PEEK plate corresponding to two sample speeds. Lower row: (a) Experimental profiles of ln(Tr) as a function of the distance to the laser spot for PEEK at several angles with respect to the direction of the sample motion, for v = 1.00 mm/s. Dots are the experimental data and the straight lines are the linear fits. (b) Experimental slopes versus angle θ corresponding to the linear fits of Fig. 6(a). The continuous line is the fit using Eq. (4).

The results we have obtained for the CFRP are shown in Fig. 7. In the left column we show the results corresponding to the sample moving in the direction of the fibers and in the right column the results for the sample moving in the direction perpendicular to the fibers. In both configuration the sample is moving at v = 5.55 mm/s. In the upper row we plot the averaged thermograms of ln(T). Note the different shape of the thermograms indicating a high thermal anisotropy. In the middle row we show the experimental profiles of ln(Tr) as a function of the distance to the laser spot for several angles θ. Dots are the experimental data and the continuous lines are the linear fits from which the slopes are obtained. Finally, in the lower row we plot the fitted slopes as a function of the angle θ together with the fitting using Eq. (8). It is worth mentioning the different shape of both curves, as it was predicted in Fig. 3a. From each fitting we retrieved the two in-plane principal diffusivities. From Fig. 7e, we obtained $D_{||}$ = 2.8 ± 0.2 mm^2/s and $D_{\perp}$ = 0.41 ± 0.04 mm^2/s, whereas from Fig. 7f, we got $D_{||}$ = 2.7 ± 0.6 mm^2/s and $D_{\perp}$ = 0.49 ± 0.03 mm^2/s. Here $||$ and $\perp$ mean parallel and perpendicular to the fibers, respectively. These values are consistent and agree with the values obtained using a lock-in laser-spot thermography setup, where the sample remains at rest and is illuminated by a modulated laser beam. Anyway, note the high uncertainty of the results corresponding to the $D_{||}$ when the sample is moving in the direction perpendicular to the fibers. This drawback is not a limitation of our experimental setup, but it is intrinsic to the linear method as it was confirmed using synthetic data with added random noise. We have repeated the same procedure for v = 2.35 mm/s. All thermal diffusivity values are summarized in Table 1.

In Fig. 8 we show the results for the same CFRP plate but moving in two directions not coincident with any principal axis, but making angles ψ = 30.0 ± 0.5º and 60.0 ± 0.5º between the direction of the sample motion and the fibers. The aim is to obtain simultaneously the two in-plane thermal diffusivities and the angle ψ. In the left column we show the results for ψ = 30º and in the right column the results for ψ = 60º. In both orientations the sample is moving at v = 5.55 mm/s. In the upper row we plot the averaged thermograms of ln(T) where the lack of symmetry stands out. In the middle row we show the experimental profiles of ln(Tr) as a function of the distance to the laser spot for several angles α, which is the angle between the direction of the sample motion and the temperature profile (see Fig. 1b). As in previous plots, dots are the experimental data and the continuous lines are the linear fits from which the slopes are obtained. Finally, in the lower row we plot the fitted slopes as a function of the angle α together with the fitting using Eq. (11). From Fig. 8e, we obtained $D_{||}$ = 2.7 ± 0.2 mm^2/s, $D_{\perp}$ = 0.40 ± 0.04 mm^2/s and ψ = 28.6 ± 1.4º, whereas from Fig. 8f, we got $D_{||}$ = 2.9 ± 0.4 mm^2/s, $D_{\perp}$ = 0.42 ± 0.03 mm^2/s and ψ = 61.0 ± 1.1º. Note the consistency of the retrieved values of the principal diffusivities and of the fibers direction. In Table 2 we summarize the results obtained for the principal thermal diffusivities and the orientation of the principal axes for the four orientations of the fibers analyzed in this work, ψ = 0º, 30º, 60º and 90º.

The multi-linear fitting proposed in this work makes use of a very high percentage of the information gathered in the thermogram, which reduces eventual systematic errors associated to the evaluation of the thermal diffusivity from two single profiles. These profiles, typically horizontal and vertical, coincide with the structure of the Focal Plane Array of the IR camera, and are more likely to be affected by diffraction effects. Moreover, the proposed approach provides generality as neither knowledge of the direction of the principal axes, nor coincidence of the direction of motion with one of the principal directions is needed. The method is thus significantly more robust, general and powerful than the one presented in [8].

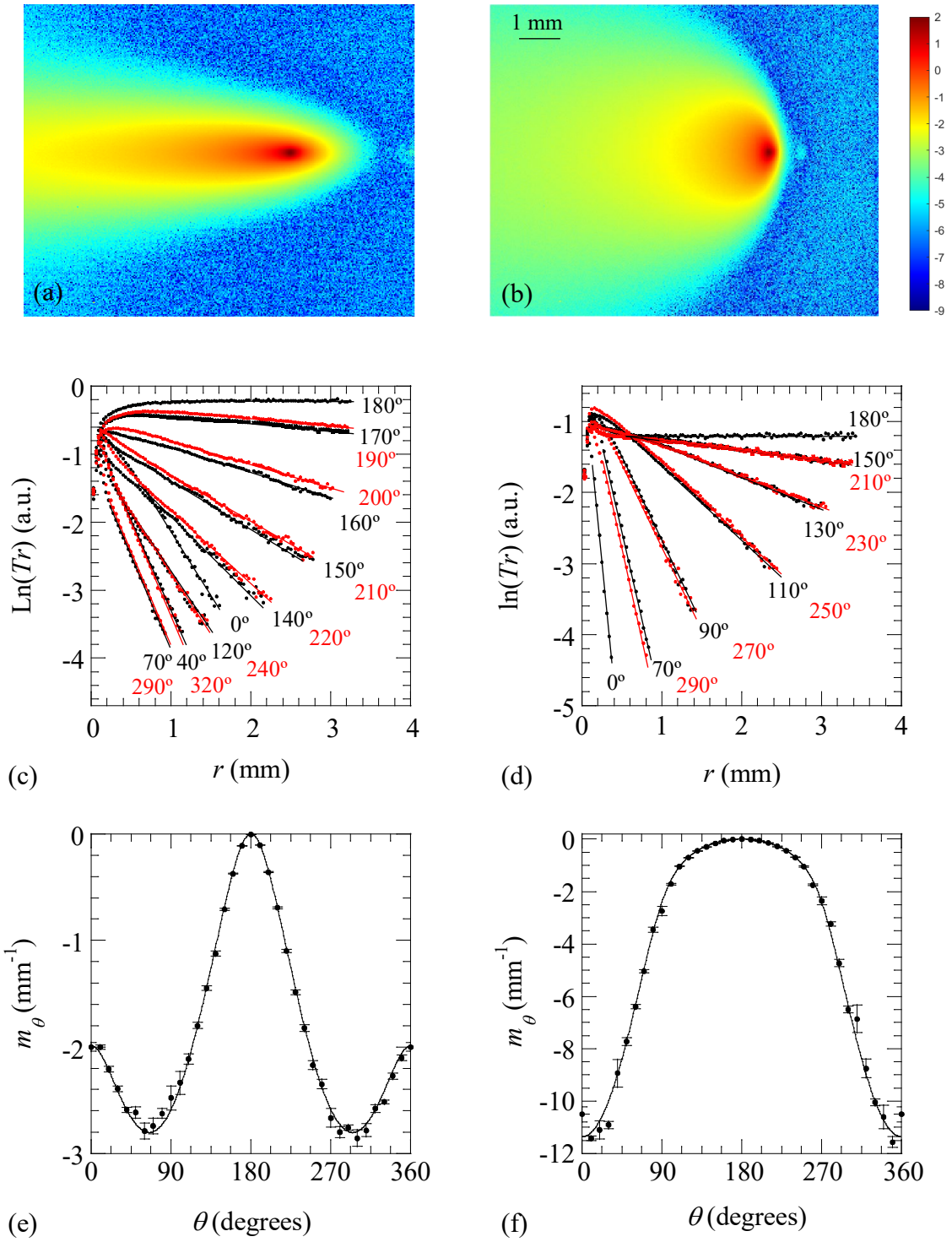

Fig. 7. Upper row: averaged thermograms of ln(T) for a CFRP sample moving at 5.55 mm/s. (a) The sample is moving along the fibers direction, (b) the sample is moving in the perpendicular direction. Middle row: Experimental profiles of ln(Tr) as a function of the distance to the laser spot for CFRP at several angles with respect to the direction of the sample motion, for v = 5.55 mm/s. Dots are the experimental data and the straight lines are the linear fits. (c) v is parallel to the fibers, (d) v is perpendicular to the fibers. Lower row: Experimental slopes versus angle θ corresponding to the linear fits of Fig. 7(c) and (d). The continuous line is the fit using Eq. (8). (e) v is parallel to the fibers, (f) v is perpendicular to the fibers.

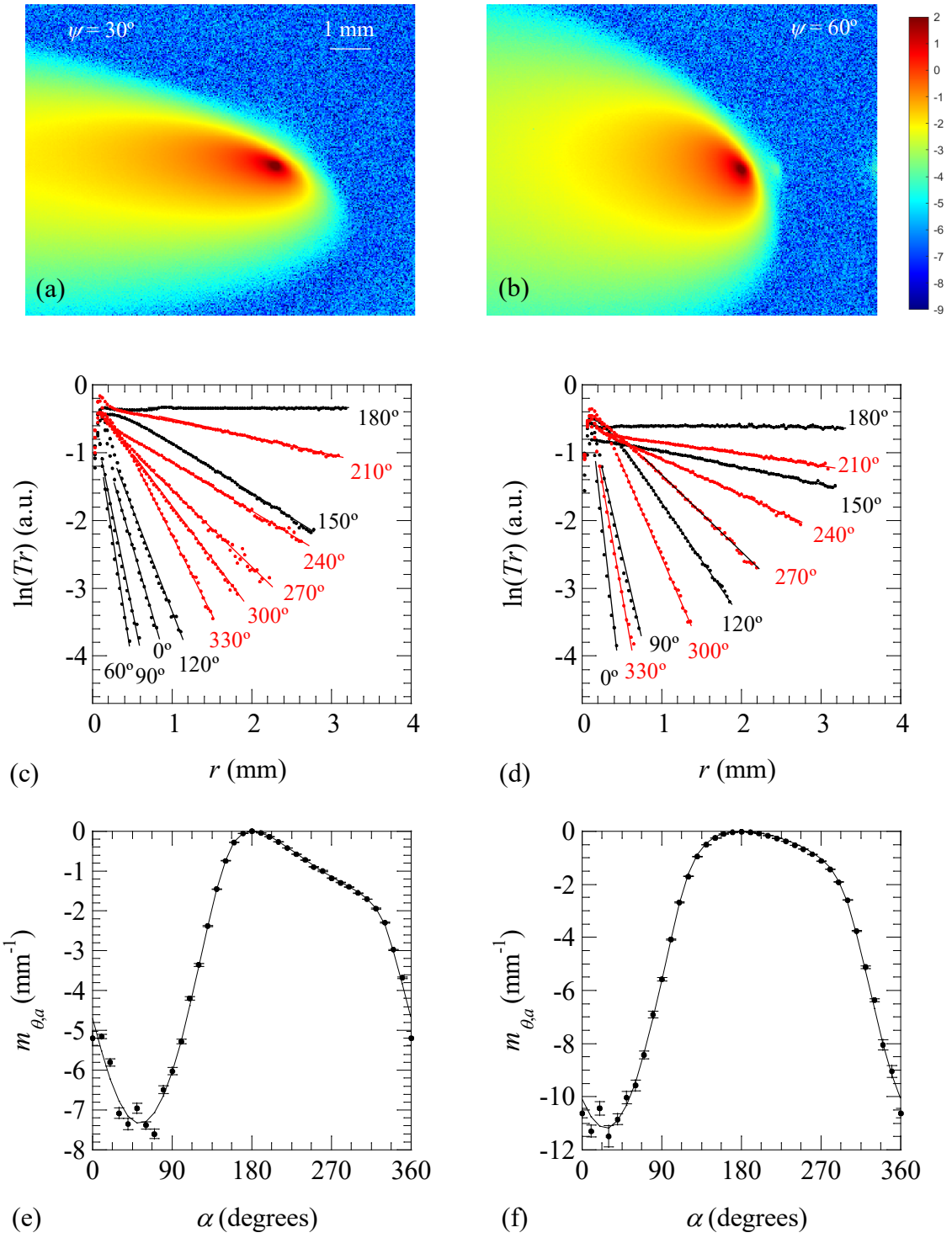

Fig. 8. Upper row: averaged thermograms of ln(T) for a CFRP sample moving at 5.55 mm/s. The sample is moving along a direction making an angle (a) $\psi = 30º$ and (b) $\psi = 60º$ with respect to the fibers. Middle row: Experimental profiles of ln(Tr) as a function of the distance to the laser spot at several angles α with respect to the direction of the sample motion for (c) $\psi = 30º$ and (d) $\psi = 60º$. Dots are the experimental data and the straight lines are the linear fits. Lower row: Experimental slopes versus angle α corresponding to the linear fits of Fig. 8(c) and (d). The continuous line is the fit using Eq. (11).

Table 1. Summary of the obtained thermal diffusivity values for the three reference samples studied in this work.

Material	v (mm/s)	D (mm^2/s) This work	D (mm^2/s) Literature[17,18]
PEEK	0.49	0.22 ± 0.01	0.20
PEEK	1.00	0.21 ± 0.01	0.20
PEEK	4.30	0.22 ± 0.02	0.20
AISI-304	5.50	3.8 ± 0.2	4.0
AISI-304	10.9	4.1 ± 0.2	4.0
AISI-304	21.4	4.0 ± 0.2	4.0
AISI-304	41.2	3.8 ± 0.2	4.0
AISI-304	60.4	4.1 ± 0.3	4.0
AISI-304	81.6	4.2 ± 0.3	4.0
CFRP	2.35 (∥ fibers)	$D_{\parallel}$ = 2.9 ± 0.2 $D_{\perp}$ = 0.39 ± 0.04	2.9 ± 0.1 0.40 ± 0.02
CFRP	2.35 (⊥ fibers)	$D_{\parallel}$ = 2.8 ± 0.5 $D_{\perp}$ = 0.43 ± 0.02	2.9 ± 0.1 0.40 ± 0.02
CFRP	5.55 (∥ fibers)	$D_{\parallel}$ = 2.8 ± 0.2 $D_{\perp}$ = 0.41 ± 0.04	2.9 ± 0.1 0.40 ± 0.02
CFRP	5.55 (⊥ fibers)	$D_{\parallel}$ = 2.7 ± 0.6 $D_{\perp}$ = 0.42 ± 0.03	2.9 ± 0.1 0.40 ± 0.02

Table 2. Summary of the obtained principal thermal diffusivities and orientation of the principal thermal directions in CFRP moving at 5.55 mm/s for different angles of the fibers with the direction of motion, ψ.

ψ (true)	ψ (estimated)	D (mm^2/s) This work	D (mm^2/s) Literature[17,18]
0º	-0.45 ± 0.2º	$D_{\parallel}$ = 2.8 ± 0.2 $D_{\perp}$ = 0.41 ± 0.04	2.9 ± 0.1 0.40 ± 0.02
30º	28.6 ± 1.4º	$D_{\parallel}$ = 2.7 ± 0.2 $D_{\perp}$ = 0.40 ± 0.04	2.9 ± 0.1 0.40 ± 0.02
60º	61.0 ± 1.1º	$D_{\parallel}$ = 2.9 ± 0.4 $D_{\perp}$ = 0.42 ± 0.03	2.9 ± 0.1 0.40 ± 0.02
90º	89.4 ± 1.1º	$D_{\parallel}$ = 2.7 ± 0.6 $D_{\perp}$ = 0.42 ± 0.03	2.9 ± 0.1 0.40 ± 0.02

4. CONCLUSIONS

As a summary, we have developed a general, robust and reliable method to measure the thermal diffusivity of samples moving at constant speed using laser-spot thermography with continuous illumination. We have presented analytical expressions of the surface temperature for both isotropic and anisotropic materials illuminated by a tightly focused, continuous-wave laser spot and we have shown that the natural logarithm of the radial temperature profiles (multiplied by the radial distance) fulfil linear relationships with the distance. We have obtained the analytical dependence of these straight lines with the thermal diffusivity, the speed and the orientation of the profile with respect to the sample motion. The proposed method involves the linear fitting of these radial profiles and the subsequent fitting of the slopes as a function of the orientation of the profile with the direction of motion.

The method is simple as it only involves linear fittings of the temperature profiles crossing the center of the laser spot and an additional simple nonlinear fit. On the other hand, it makes use of the whole surface temperature distribution, which provides robustness against systematic errors, improving the accuracy. Moreover, the signal-to-noise ratio can be enhanced by averaging a number of thermograms, thus improving the precision of the method. The principal diffusivities have been determined with high accuracy and uncertainties of about 5%. Only when the sample moves parallel to the low diffusivity principal direction, the uncertainty in the high principal diffusivity reaches 20%. However, the most significant contribution is the treatment of anisotropic materials. The restriction associated to previous methodologies, regarding the need of knowledge of the principal direction but especially the need of coincidence between the direction of the sample motion and one of the principal directions are not compulsory requirements anymore. As a matter of fact, the method is able to identify the principal directions with accuracy of about 1º, which proves a remarkable reliability. This might be significantly useful for in-line quality control of anisotropic products in which the principal directions make arbitrary (and unknown) angles with the motion of the chain. For instance, the method could be useful for implementing fiber orientation control in CFRP, or for an accurate assessment of homogeneity of the thermal properties of the product.

Acknowledgments

This work has been supported by Ministerio de Ciencia e Innovación (PID2019-104347RB-I00, AEI/FEDER, UE), by Gobierno Vasco (PIBA 2018-15) and by Universidad del País Vasco UPV/EHU (GIU19/058).

REFERENCES

[1] B. Abad, D.A. Borca-Tasciuc and M.S. Martin-Gonzalez, Non-contact methods for thermal properties measurement, Renew. Sustain. Ebergy Rev. 76, 1348-1370 (2017).
[2] A. Salazar, A. Mendioroz and A. Oleaga, Flying spot thermography imaging: quantitative assessment of thermal diffusivity and crack width, J. Appl. Phys. **127**, 131101 (2020).
[3] L. Fabbri and P. Fenici, Three-dimensional photothermal radiometry for the determination of the thermal diffusivity of solids, Rev. Sci. Instrum. **66**, 3593-3600 (1995).
[4] B. Zhang and R. E. Imhof, Theoretical analysis of the surface thermal wave technique for measuring the thermal diffusivity of thin plates, Appl. Phys. A, **62**, 323-334 (1996).
[5] F. Cernuschi, A. Russo, L. Lorenzoni, A. Figari, In-plane thermal diffusivity evaluation by infrared thermography, Rev. Sci. Instrum. **72**, 3988 (2001).
[6] E. Ruffio, D. Saury, D. Petit, Improvement and comparison of some estimators dedicated to thermal diffusivity estimation of orthotropic materials with the 3d-flash method, Int. J. Heat. Mass. Transf. **64**, 1064-1081 (2013).
[7] W. Adamczyk, R. Białecki, H. R.B. Orlande and Z. Ostrowski, Nondestructive, real time technique for in-plane heat diffusivity measurements, Int. J. Heat. Mass. Transf. **154**, 119659 (2020).
[8] A. Bedoya, J. González, J. Rodríguez-Aseguinolaza, A. Mendioroz, A. Sommier, J.C. Batsale, C. Pradere and A. Salazar, Measurement of in-plane thermal diffusivity of solids moving at constant velocity using laser spot infrared thermography, Measurement **134**, 519-526 (2019).
[9] A. Bedoya, J. González, A. Mendioroz, C. Pradere, A. Sommier, J. C. Batsale and A. Salazar, Flying-spot thermography: measuring the in-plane (an)isotropic thermal diffusivity of large and complex parts, Proceedings of SPIE Vol. **11004**, 110040J (2019).
[10] M. Colom, A. Bedoya, A. Mendioroz and A. Salazar, Measuring the in-plane thermal diffusivity of moving samples using laser spot lock-in thermography, Int. J. Thermal Sci. **151**, 106277 (2020).
[11] A. Salazar, L. Zamanillo, M. Colom, A. Mendioroz, U. Galietti, A. Sommier, J.C. Batsale and C. Pradere, Lock-in thermography on moving samples: amazing mismatch between amplitude and phase, QIRT J. **17**, 179-286 (2020).
[12] L. Gaverina, J.C. Batsale, A. Sommier and C. Pradere, Pulsed flying spot with logarithmic parabolas method for the estimation of on-plane thermal diffusivity fields on heterogeneous and anisotropic materials, J. Appl. Phys. **121**, 115105 (2017).
[13] L. Gaverina, A. Sommier, J.L. Battaglia, J.C. Batsale and C. Pradere, Pulsed flying spot elliptic method for the estimation of the thermal diffusivity field of orthotropic materials, Int. J. Thermal Sci. **125**, 142-148 (2018).
[14] A. Sommier, J. Malvaut, V. Delos, M. Romano, T. Bazire, J.C. Batsale, A. Salazar, A. Mendioroz, A. Oleaga and C. Pradere, Coupling Pulsed Flying Spot technique with robot automation for industrial thermal characterization of complex shape composite materials, NDT&E Int. **102**, 175-179 (2019).
[15] L. Gaverina, M. Bensalem, A. Bedoya, J. González, A. Sommier, J.L. Battaglia, A. Salazar, A. Mendioroz, A. Oleaga, J.C. Batsale and C. Pradere, Constant Velocity Flying Spot for the estimation of in-plane thermal diffusivity on anisotropic materials, Int. J. Thermal Sci. **145**, 106000 (2019).
[16] H.S. Carslaw and J.C. Jaeger, *Conduction of Heat in Solids*, 2nd edition (Oxford University Press, 1959).
[17] Y.A. Çengel, Heat Transfer: A practical Approach (McGraw-Hill, Boston, 2003).
[18] Goodfellow catalogue at http://www.goodfellow.com.